Journal of Geoscience and Environment Protection, 2025, 13(8), 27-43
https://www.scirp.org/journal/gep
ISSN Online: 2327-4344
ISSN Print: 2327-4336

Evaluation and Application of Roadway Surrounding Rock Stability Based on Comprehensive Index Method

Jicheng Feng[1], Zhihai Ji[1], Xiangye Wu[2], Jianjun Shi[1], Chaoyang Dong[1], Gexuan Niu[1], Yanqi Gao[1]

[1]Mine Safety Institute, North China University of Science and Technology, Langfang, China
[2]School of Mining and Coal, Inner Mongolia University of Science and Technology, Baotou, China
Email: 1229840418@qq.com

How to cite this paper: Feng, J. C., Ji, Z. H., Wu, X. Y., Shi, J. J., Dong, C. Y., Niu, G. X., & Gao, Y. Q. (2025). Evaluation and Application of Roadway Surrounding Rock Stability Based on Comprehensive Index Method. *Journal of Geoscience and Environment Protection, 13,* 27-43.
https://doi.org/10.4236/gep.2025.138002

Received: June 22, 2025
Accepted: August 15, 2025
Published: August 18, 2025

Abstract

In order to scientifically and quantitatively evaluate the stability of the perimeter rock of the roadway in Baliancheng coal mine, this paper adopts a comprehensive method of field measurement, theoretical analysis, laboratory test and numerical simulation to study the geological and structural characteristics of the perimeter rock of the roadway, the physical and mechanical properties of the perimeter rock as well as the state of the perimeter rock stress, and proposes a comprehensive index method for classifying the stability of the perimeter rock of the roadway. The research results show that: the top plate of 18 coal roadway is mainly medium-hard rock composite top plate of siltstone, medium-grained sandstone and coarse sandstone, and the bottom plate is soft-medium-hard rock composite bottom plate of medium-grained sandstone, fine-grained sandstone and coarse-grained sandstone, the coefficient of coal seam solidity is 1.28, the fissures of perimeter rock are moderately developed, the influence coefficient of mining is 2.71, and the ratio of the maximal horizontal principal stress to the vertical stress is 1.90, the stability grade of 18 coal roadway perimeter rock belongs to medium stable perimeter rock, after adopting the optimized support scheme, the overall deformation of the roadway is relatively reduced compared with the original support scheme, and the support effect of the roadway perimeter rock is good.

Keywords

Geological Structure, Physical Properties, Stress State, Stability Classification, Support Scheme

1. Introduction

The discernment of the destabilization damage of the roadway surrounding rock mainly depends on the geological state, structural characteristics and integrity of the surrounding rock, the physical and mechanical properties of the rock, and the stress environment (Li et al., 2022; Yang & Liu, 1999; Zhao et al., 2024). The classification of surrounding rock stability is an important basis for engineering design and the formulation of corresponding engineering measures, and with the deep mining of coal, the stability of the roadway surrounding rock plays a key role in the construction of safe and efficient mines (Cheng & Wu, 2022; Dong et al., 2023; Feng, 2022; Lan et al., 2022).

For a long time, many experts and scholars at home and abroad for the stability of the surrounding rock research have done a lot of work, Hou Chaojiong, et al (Hou et al., 1997) put forward a gently sloping and inclined coal seam back to mining roadway rock stability classification method, to determine the selection of the roadway roof strength, the strength of the bottom plate, the strength of the coal seam, the depth of the roadway, the direct top of the first fall step, the thickness of the direct top of the ratio of the mining height, the width of coal protection of the seven main factors affecting the stability of roadway in mining areas. As a classification index for evaluating the stability of the roadway, Xu & Li (2020) established a fuzzy comprehensive judgment mathematical model, and selected the above seven factors to evaluate the stability of the roadway; Zhang Peisen et al. (Zhang et al., 2023) constructed a formula for destroying the depth of the bottom plate with the depth of mining, mining height, sloping length of the working face, and the inclination angle of the coal seam as the influencing factors by the use of grey correlation analysis (GRA) and multivariate regression statistics, and predicted the stability of the roadway; Xu & Li (2020) used the fuzzy comprehensive judgment method to establish a model, selected the surrounding rock's own nature and the stress environment and other factors to classify the roadway stability, and used the gray correlation method to verify; Cao Rongguo et al. (Cao & Hu, 2024) used the use of the Q-system perimeter rock classification, the RMR method, and the engineering geology classification method to classify the perimeter rock stability of the red layer soft rock tunnels, respectively; furthermore, some scholars have employed fuzzy clustering analysis (Lian et al., 2023; Wei et al., 2010; Zheng & Yu, 2014) to classify roadway samples, applied this method to evaluate the stability of surrounding rock, and subsequently quantified the influencing factors of roadway stability through multiple stepwise regression analysis (Zhang et al., 2016; Zhu et al., 2015) to quantify and analyze the various stability factors of the roadway surrounding rock. However, due to the characteristics of the roadway surrounding rock, the stress environment and the complexity of the geological environment is limited to the qualitative analysis basis. It is difficult to accurately analyze and predict the stability of the surrounding rock of the timeliness, mostly based on the experience of the fuzzy qualitative evaluation, the lack of a unified quantitative judgment index.

Therefore, this paper takes the actual engineering geological conditions of the 18 coal seams in Baliancheng Coal Mine as the background, obtains the classification indexes affecting the stability of the surrounding rocks of the roadway from the field practice, researches the geological and structural characteristics of the surrounding rocks of the roadway, the physical and mechanical properties of the surrounding rocks as well as the stress state of the surrounding rocks, and puts forward the comprehensive index method of the classification of the stability of the surrounding rocks of the roadway, and combines the classification results of the stability of the surrounding rocks of the roadway of the gently sloping and inclined seams with those of the backmining roadway. Combined with the classification results of gently sloping and inclined coal seam, the method is used to scientifically and quantitatively evaluate the stability of the surrounding rocks in the roadway of Baliancheng Coal Mine, and to design an optimized support scheme based on the classification results.

2. Characteristics of the Geological Structure of the Roadway Surrounding Rock

2.1. Coring of Coal Rock

In the unmined disturbed area of the west three areas protruding appraisal of the No. 5 roadway 18 coal top and bottom plate each take 10 m rock core, study the roadway top and bottom plate of the location of different rock layers and layering thickness, access to the roadway perimeter rock structural combination of characteristics, so as to carry out the physical and mechanical properties of the rock of each rock layer test, the top and bottom plate rock core is shown in (Figure 1).

rock name	histogram	thicknesses /m	Drilling depth/m
sandy mudstone		0.41	10.0
coarse-grained sandstone		0.59	9.59
coarse-grained sandstone		0.86	8.86
sandy mudstone		0.29	8.0
coarse-grained sandstone		0.71	7.71
siltstone		1.0	7.0
coarse-grained sandstone		0.66	6.0
medium-grained sandstones		0.34	5.34
coarse-grained sandstone		0.46	5.0
medium-grained sandstones		0.54	4.54
coarse-grained sandstone		1.57	4.0
medium-grained sandstones		2.43	2.43

(a) 18 Coal roof coring photos and roof rock layer histograms

rock name	histogram	thicknesses /m	Drilling depth/m
sandy mudstone		0.37	0.59
medium-grained sandstones		0.95	1.54
coarse-grained sandstone		0.46	2.0
medium-grained sandstones		2.0	4.0
Fine-Grained Sandstones		2.0	6.0
medium-grained sandstones		1.17	7.17
coarse-grained sandstone		0.83	8.0
medium-grained sandstones		1.19	9.19
silty mudstone		0.81	10.0

(b) 18 Coal floor coring photographs with floor rock strata histograms

Figure 1. Characteristics of the structural combination of roof and floor rock strata in the roadway.

From (**Figure 1(a)**), it can be seen that the 18-coal roof slab core is light gray, medium cementation, medium sorting, dominated by quartz and rock fragments in the range of 0 - 2.43 m drilling core, judged as medium-grained sandstone, and the integrity of this section of the core is poor in the range of 0 - 1.3 m due to the periphery of the roadway. There are two sections larger than 20 cm in the whole section: 4.0 - 4.54 m and 5.0 - 5.34 m. These two sections are also judged to be medium-grained sandstones. These two sections are broken, and only one section of the core is larger than 10 cm. Within the range of core 2.43 - 4.0 m, the rock is mainly grayish white, with medium cementation and poor sorting, and the composition is dominated by quartz, feldspar, and metamorphic rocks, which is judged to be a conglomerate-bearing coarse-grained sandstone, and within the range of the whole section, there are four sections of greater than 10 cm, with the cores being more broken, and the rest of the cores being more complete and more of them are short columns, 4.54 - 5.0 m, 5.34 - 6.0 m, 7.0 - 7.0 m, 7.0 - 7.0 m, and 7.0 - 7.0 m. 4.54 - 5.0 m, 5.34 - 6.0 m, 7.0 - 7.71 m, 8.0 - 8.86 m are also judged as coarse-grained sandstone. The whole is relatively broken, and there are 6 sections with cores larger than 10 cm; the rocks in core 6.0 - 7.0 m are mainly gray, moderately cemented, and contain charcoal compounds. This is judged to be siltstone with good integrity. The last 0.4 m is broken overall, brownish black, massive, containing a lot of charcoal compounds, and is judged to be mudstone; core 9.59 - 10.0 m is dark gray, massive, containing charcoal debris, and is judged to be silty mudstone. The core is dark gray, blocky, with carbonaceous debris, and judged to

be siltstone. The whole is relatively broken, and there is no core over 10 cm.

From (Figure 1(b)), it can be seen that the first 4 m of the core is overall more broken, and there are only 4 segments larger than 10 cm. Within the range of 0 - 0.22 m, 1.54 - 2.0 m, 7.17 - 8.0 m of the core of the 18-coal bottom plate, the rocks are mainly grayish-white, with medium cementation and poor sorting, and the constituents are dominated by quartz, feldspar, and metamorphic rocks, and are judged to be conglomerate - bearing coarse - grained sandstones, and there are 2 segments larger than 10 cm in the whole range of the section. The cores 0.59 - 1.54 m, 2.0 - 4.0 m, 6.0 - 7.17 m, 8.0 - 9.19 m are light gray, moderately cemented, moderately sorted, and dominated by quartz and rock fragments, which are judged to be medium-grained sandstones, and the cores, due to the fact that they are in the roadway, are larger than 30 cm in the entire range of 1 section, and there are only 3 sections of the cores that are larger than 10 cm. Within the range of 0.22 - 0.59 m and 9.19 - 10.0 m, the core is dark gray, blocky, containing charcoal debris, and is judged to be silty mudstone. The whole is relatively broken, and there are no cores of more than 10 cm.

2.2. Fine Detection of Roadway Roof

Two 8m top plate drill holes were drilled in No.3 lane of West Zone 3 for peeping. No.1 and No.2 drill holes were peeped as shown in (Figure 2).

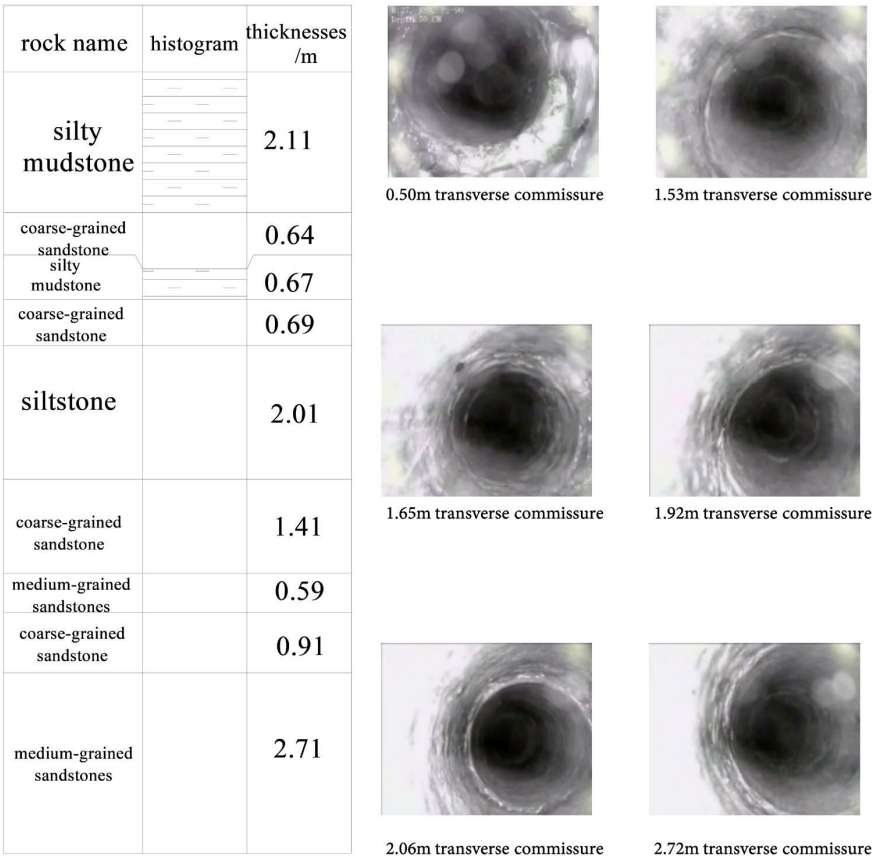

(a) Roof plate 1 drill hole peep results

rock name	histogram	thicknesses /m
silty mudstone		1.51
coarse-grained sandstone		1.60
siltstone		2.60
coarse-grained sandstone		1.07
medium-grained sandstones		0.73
coarse-grained sandstone		1.41
medium-grained sandstones		2.76

0.05m junction gap

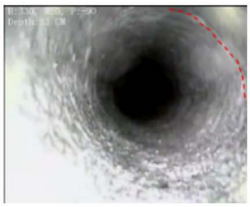

0.33m mtransverse commissure

2.16m mtransverse commissure

(b) Roof plate 2 drill hole peep results

Figure 2. Results of borehole inspection for the roof.

From (**Figure 2(a)**), it can be seen that the rock structure is more complicated, which are medium-grained sandstone, coarse-grained sandstone and siltstone. The stability of the roof is good, the transverse fissures mainly appear in the range of 0 - 3 m, which are prone to delamination, and the transverse fissures can be seen at the positions of 0.5 m, 1.53 m, 1.65 m, 1.92 m, 2.06 m, and 2.72 m. The rest of the positions are more intact, and the fissures are moderately developed.

From (**Figure 2(b)**), it can be seen that the rock structure is more complicated, which are medium-grained sandstone, coarse-grained sandstone and siltstone mudstone. The stability of the roof is good, the transverse fissures mainly appear in the range of 0 - 3 m, which is easy to occur off the layer, the transverse fissures can be seen at the position of 0.05 m, 0.33 m, 2.16 m, the rest of the position is more intact, the fissures are moderately developed.

3. Physical and Mechanical Properties of Roadway Surrounding Rock

In accordance with the requirements stipulated in the standard "Determination of Physical and Mechanical Properties of Coal and Rock GT/T23561-2009", obtained through laboratory coal rock sample experiments, the main parameters for

the true density of coal and rock, apparent density, uniaxial tensile strength, uniaxial compressive strength, modulus of elasticity, Poisson ratio, cohesion, angle of internal friction and so on, the results of the determination of the details are shown in (Table 1).

Table 1. Physical and mechanical parameter measurements of the surrounding rock in No. 18 coal seam roadway in Bachenglian Coal Mine.

lithology	apparent density (g/cm^3)	compressional strength (Mpa)	modulus of elasticity (GPa)	Poisson ratio	tensile strength (MPa)	Cohesion (MPa)	angle of internal friction (o)
coarse-grained sandstone (top)	2.40	28.83	7.71	0.31	0.76	4.02	31.53
siltstone (top)	2.65	41.84	17.80	0.28	1.77	5.89	37.62
medium-grained sandstones (top)	2.33	25.65	8.02	0.43	1.15	4.80	34.32
18 Coal	1.27	12.77	3.02	0.43	0.62	2.93	27.92
medium-grained sandstones (floor)	2.34	24.72	8.59	0.41	1.08	4.61	33.17
Fine-Grained Sandstones (floor)	2.42	27.30	8.35	0.27	1.07	5.77	38.16
coarse-grained sandstone (floor)	2.41	27.87	6.74	0.32	0.81	4.13	31.76

4. Stress State of Roadway Surrounding Rock

4.1. Geostress Testing

The geostress measurement adopts the original geostress measurement method of hydraulic fracturing, and the borehole is drilled vertically upward at the guide point of S17 in No.3 lane of No.18 coal in Baliancheng coal mine, the depth of the borehole opening is 632 m. The 3 measurement holes are 10 m apart, and 1 section of fracturing measurement is carried out in each hole. In the measured hole test, the rupture pressure, retensioning pressure and closure pressure in all measured holes can be clearly seen in each cycle, and the repeatability is relatively good. Therefore, the maximum horizontal principal stress and the minimum horizontal principal stress at each section could be calculated from the retension pressure and the closure pressure, respectively. Then the vertical stress (S_V) value of each section was obtained according to the thickness of the overlying rock layer and the rock bulk weight (2.5 g/cm^3). The detailed results of the three holes are shown in (Figure 3) and (Table 2).

According to the data in Table 2, the maximum horizontal principal stress (S_H) is 18.6 - 22.8 MPa, the minimum horizontal principal stress (S_h) is 10.22 - 11.68 MPa, and the vertical principal stress (S_V) is 15.47 MPa. It can be seen that the horizontal stress is dominant at this location, and $S_H > S_V > S_h$. The measured

lateral pressure coefficient ranges from 1.20 to 1.47, with an error margin of 0 - 0.27, demonstrating negligible influence on the stability classification.

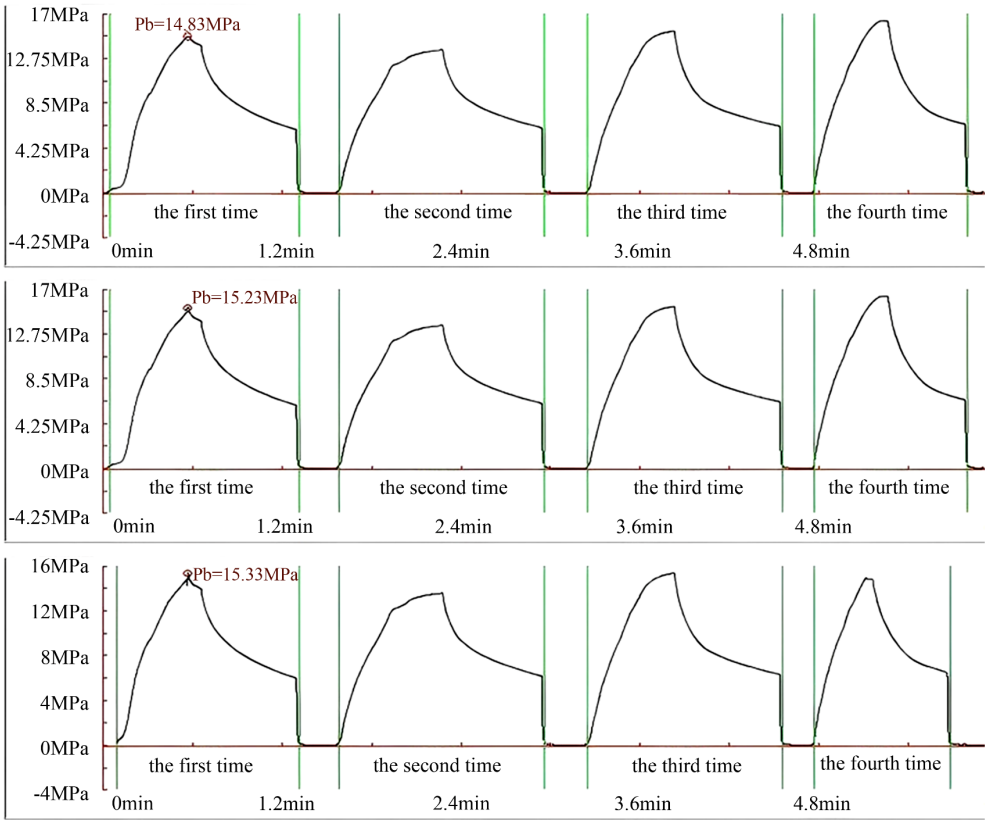

Figure 3. Pressure variation curve for the three measurement sections at the measurement point.

Table 2. Hydraulic fracturing stress measurement results from three boreholes.

stoma number	Depth of section (m)	Fracturing parameters			Principal stress value (MPa)		
		Breakdown pressure P_b	Reopening pressure P_r	Closing pressure P_s	SH	Sh	Sv
1	632	14.83	12.15	11.17	21.36	11.17	15.47
2		15.23	11.96	10.22	18.60	10.22	
3		15.33	12.16	11.68	22.80	11.68	
average value (MPa)					20.92	11.02	15.47

Annotation: [1]P_b—*In-situ* rock breakdown pressure; [2]P_r—Rupture surface reopening pressure; [3]S_s—Rupture surface closing pressure; [4]S_h—Horizontal minimum principal stress; [5]S_H—Horizontal maximum principal stress; [6]S_v—Vertical principal stress; [7]The vertical stress S_v is calculated by taking the bulk weight of the overlying rock as: 2.5 g/cm^3.

Using borehole imaging technology, the significant rupture directions of the three test holes can be observed as shown in (Figure 4), and the directions of the maximum horizontal principal stresses S_H are determined to be N45.85˚E, N29.69˚E and N39.32˚E, respectively.

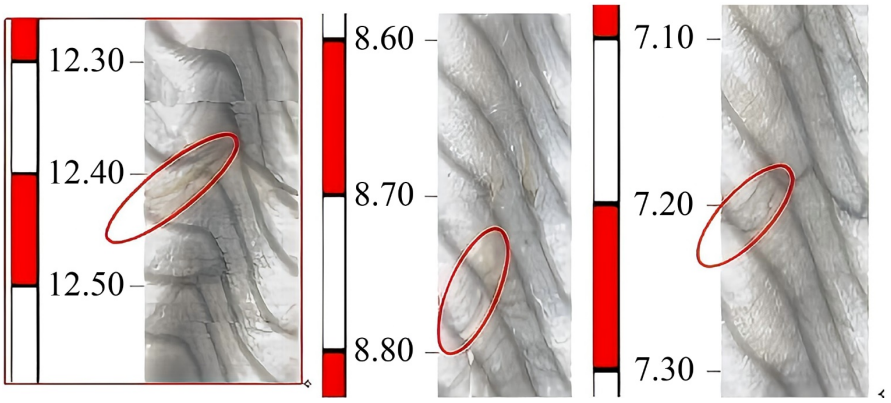

Figure 4. Fracture patterns observed during hydraulic fracturing at measurement point three.

4.2. Mining Stress Distribution

Based on the engineering conditions of Baliancheng coal mine, FLAC3D was used to simulate the mining work of the 18 coal seam to obtain the evolution law of the mining stress field in the process of 18 coal seam back mining.

1) Modeling. The FLAC3D computer model was established with the top and bottom plate of the 18 coal seam in Baliancheng coal mine, and the model size was 400 m × 500 m × 282 m. The x-direction was used as the tendency of the working face, and the y-direction was the direction of the working face. The model contains 1,160,502 nodes and 1,128,370 hexahedral elements. The bottom boundary was fixed with displacement constraints, while the lateral boundaries (x and y directions) were assigned normal displacement constraints. A vertical stress of 9.725 MPa was applied to simulate the overburden pressure. The Mohr-Coulomb constitutive model was adopted with a unit weight of 2.5 kg/m^3. Based on in-situ stress measurements, the lateral pressure coefficients were determined as 1.4 and 1.2 for the X and Y directions, respectively. The mechanical parameters of coal and rock strata were assigned according to laboratory test results, employing the Mohr-Coulomb failure criterion. The initial stress field was balanced to calibrate both the magnitude and orientation of stresses. Subsequent excavation simulations were performed to analyze the abutment pressure distribution around the working face. The simulated results were validated against field measurements to ensure accuracy.

During mining, the roof plate at the back of the working face collapses with the advancement of the working face, and goaf is filled with a large amount of bubbling rock, which is compacted under the influence of overburden loading, forming a support for the fissure zone. For this reason, when the numerical simulation is carried out, the bubbling zone after the hollowing is filled first, and the collapsed zone is filled with a double yield model.

2) Mining stress distribution law. Coal and rock in the natural state there is a certain stress state, basically in equilibrium, by mining disturbance, coal and rock stress redistribution, the formation of mining stress.18 coal seam working face

maximum width of 190 m, excavation simulation after over the front mining stress cloud and stress curve shown in (Figure 5, Figure 6).

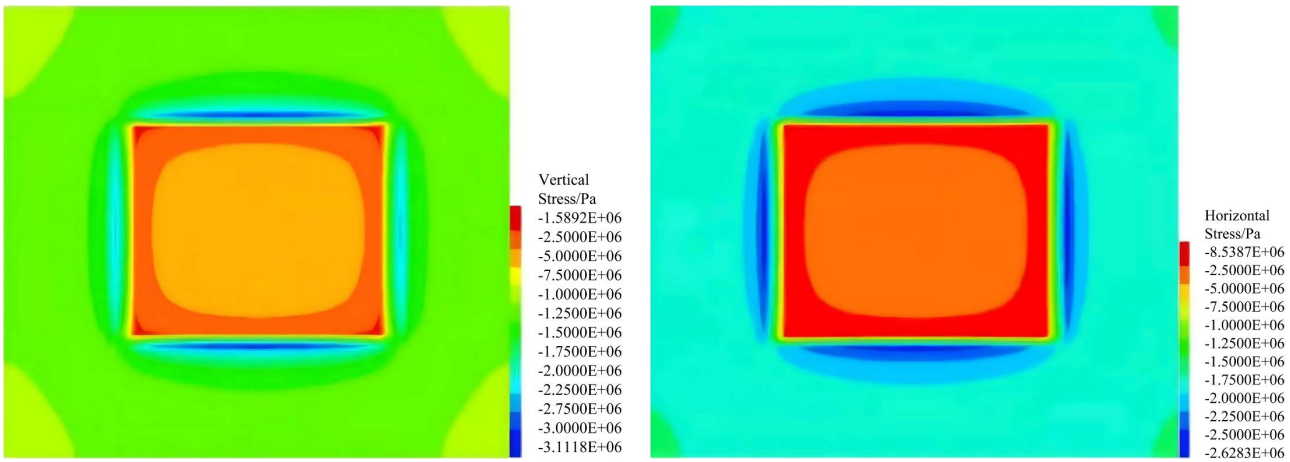

(a) Vertical stress map (b) Horizontal stress map

Figure 5. Stress contour map around the goaf of the No. 18 coal seam working face.

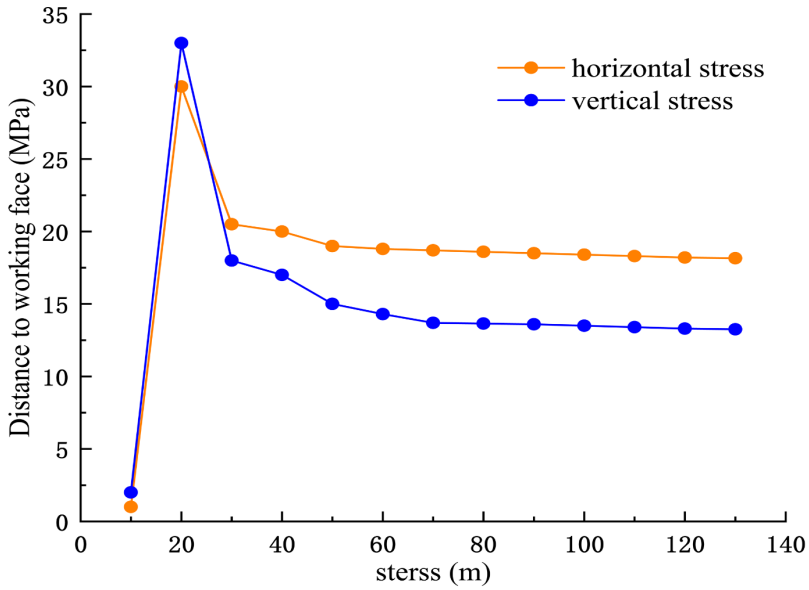

Figure 6. Advanced mining stress curve for the No. 18 coal seam working face.

From the analysis of (Figure 5, Figure 6), it can be seen that after mining the working face of 18 seam, the vertical stress and horizontal stress in front of the working face show the trend of "increase-decrease"; the change rule of vertical stress is as follows: the vertical stress in the range of 0 - 20 m in front of the working face is gradually increasing, and the peak value of the vertical stress is 32.50 MPa, which is 2.71 times of the stress in the original rock; the vertical stress in the range of 20 - 130 m in front of the working face is gradually decreasing, the stress value is 12.81 - 32.50 MPa, 1.07 - 2.71 times of the original rock stress, of which the vertical stress in the range of 20 - 30 m in the overtopping is 18.46 - 32.50 MPa,

1.54 - 2.71 times of the original rock stress; The change rule of horizontal stress is as follows: overtopping 0 - 20 m range of horizontal stress gradually increases, and the peak stress value is 30.10 MPa, which is 1.79 times of the original rock stress; the horizontal stress in the range of 20 - 130 m ahead gradually decreases, and the stress value is 17.73 - 30.10 MPa, which is 1.05 - 1.79 times of the original rock stress. To summarize, the vertical stress in the working face of 18 seam increases more obviously in the range of overtopping, and the horizontal stress increases relatively small, and the mining stress affects more obviously in the range of 0 - 24 m in the overtopping working face.

5. Classification of Roadway Surrounding Rock Stability

5.1. Comprehensive Index Method for Classifying the Stability of Roadway Surrounding Rock

1) Determine the classification index and evaluation method (Wang, 2015). Drawing on the existing classification methods, synchronously consider the key factors such as top plate strength, coal seam strength, bottom plate strength, roadway depth, coal (rock) pillar width, mining influence coefficient, perimeter rock stability index, stress ratio and so on, and put forward the comprehensive index classification method, as shown in Equation (1), which is shown in (Table 3, Table 4).

$$W_t = \frac{\sum_{i=1}^{n} W_i}{\sum_{i=1}^{n} W_{i\max}} \tag{1}$$

The comprehensive index method formula was established in accordance with the rockburst risk classification standards specified in the "Interim Measures for the Identification of Rockburst-prone Mines" (Mine Safety [2023] No. 58) issued by the National Mine Safety Administration. The weighting coefficients for roadway depth and surrounding rock stability index were determined based on Reference (Wang, 2015), while the weighting factors for roof strength, coal seam strength, floor strength, coal (rock) pillar width, mining influence coefficient, and stress ratio were derived from Reference (Bai et al., 2020).

Table 3. Stability classification table for surrounding rock in roadways.

Roadway perimeter rock stabilization grade	Steady state	Stability index
I	very stable	$W_t \leq 0.2$
II	stabilise	$0.2 < W_t \leq 0.4$
III	moderately stable	$0.4 < W_t \leq 0.6$
IV	instability	$0.6 < W_t \leq 0.8$
V	extremely unstable	$W_t > 0.8$

Table 4. Stability index evaluation table for surrounding rock in roadways.

Serial number	Factor	Description of factors	Factor classification	Rating index
1	W_1	Roof strength σ_r (MPa): Take the weighted mean of the strength of the roof slab within two times the width of the roadway	$\sigma_r > 50$	1
			$40 < \sigma_r \leq 50$	2
			$30 < \sigma_r \leq 40$	3
			$20 < \sigma_r \leq 30$	4
			$\sigma_r \leq 20$	5
2	W_2	Coal seam strength σ_c (MPa): Take a weighted mean of the strength of the coal seams in the roadway gangway	$\sigma_c > 25$	1
			$20 < \sigma_c \leq 25$	2
			$15 < \sigma_c \leq 20$	3
			$10 < \sigma_c \leq 15$	4
			$\sigma_c \leq 10$	5
3	W_3	Floor strength σ_f (MPa): Take the weighted mean of the floor strength over the width of the roadway	$\sigma_f > 50$	1
			$40 < \sigma_f \leq 50$	2
			$30 < \sigma_f \leq 40$	3
			$20 < \sigma_f \leq 30$	4
			$\sigma_f \leq 20$	5
4	W_4	Roadway Depth H (m): Vertical distance from the location of the roadway to the ground surface	$H \leq 200$	1
			$200 < H \leq 400$	2
			$400 < H \leq 600$	3
			$600 < H \leq 800$	4
			$H > 800$	5
5	W_5	Width of Coal Guard Pillar X (m): The actual width of the coal pillar on one side, where: $X = 0$ when digging along the empty roadway (no coal pillar); when both sides of the roadway are solid coal, $X = 100$	physical coal	1
			$X \leq 8$, $X \geq 50$	2
			$30 < X \leq 40$	3
			$20 < X \leq 30$	4
			$8 < X \leq 20$	5
6	W_6	Mining impact coefficient N: Impact of support pressures due to workface recovery	$N \leq 1.5$	1
			$1.5 < N \leq 2$	2
			$2 < N \leq 2.5$	3
			$2.5 < N \leq 3$	4
			$N > 3$	5

Continued

7	W_7	Surrounding rock stability index D: Refers to the degree of influence of the peripheral rock joints and fissures, laminations, non-anchor-supported work face direct top initial cross-fall steps instead of	$D > 25$	1
			$20 < D \leq 25$	2
			$15 < D \leq 20$	3
			$10 < D \leq 15$	4
			$D \leq 10$	5
8	W_8	Stress ratio λ: Ratio of maximum horizontal principal stress to vertical stress	$\lambda \leq 1.4$	1
			$1.4 < \lambda \leq 1.6$	2
			$1.6 < \lambda \leq 1.8$	3
			$1.8 < \lambda \leq 2.0$	4
			$\lambda > 2.2$	5
Stability level classification		$W_t = \frac{\sum_{i=1}^{n} W_i}{\sum_{i=1}^{n} W_{i\max}}$	$W_t \leq 0.2$	very stable
			$0.2 < W_t \leq 0.4$	stabilise
			$0.4 < W_t \leq 0.6$	moderately stable
			$0.6 < W_t \leq 0.8$	instability

2) Classification results. According to the strength of the top and bottom plates and coal seams of the Baliancheng coal mine roadway, the depth of the roadway, the direct top initial fall step, the width of the coal guarding roadway, the mining influence coefficient, the average step of the direct top initial collapse, the stress ratio and other data, to determine the classification results of the stability of the surrounding rock of the roadway of the Baliancheng coal mine, and the results of the stability class of the surrounding rock of the 18-coal roadway of the Baliancheng coal mine are all medium-stable perimeter rock shown in (Table 5).

Table 5. Classification results of surrounding rock stability in roadways of Bachenglian Coal.

coal seam	W_1	W_2	W_3	W_4	W_5	W_6	W_7	W_8	W_t	Stabilization results
18	3	4	4	3	4	4	1	1	0.6	Moderately stable

5.2. Classification of the Stability of the Surrounding Rock of the Roadway in Gently Sloping and Inclined Coal Seam Mining

In order to ensure safety and normal production, the roadway should maintain a certain stability, i.e., according to the requirements of safety regulations and technical regulations, the roadway should maintain the required shape and section size during its use. The classification method for the stability of the roadway surrounding rock in gently sloping and inclined coal seam back mining takes the strength

of the roadway top and bottom plates and coal seams (σ_D, σ_d, σ_M), the depth of the roadway (H), the direct top initial fall distance (L), the ratio of the direct top thickness to the mining height (N), and the width of the coal protection roadway (X), which are the seven main factors influencing the stability of the perimeter rock of the roadway in the mining area, as classification indexes for the evaluation of the stability of the roadway. At present, China has formulated a gently sloping and inclined coal seam back to mining roadway rock stability classification scheme table, against the determination of the Baliancheng coal mine back to mining roadway rock stability classification results (Table 6), the classification results are consistent with the comprehensive index method of roadway rock stability classification.

Table 6. Classification results of surrounding rock stability in roadways of Bachenglian Coal Mine.

roof			floor		seam strength f	jointed stratification	immediate roof Initial Collapse Mean Step Distance L (m)	Roof and floor strata		degree of stability
Rock type	σ_D (MPa)	N	Rock type	σ_d (MPa)				approach volume (%)	migration rate (mm)	
siltstone Medium-grained sandstone Coarse-grained sandstone	25.56 - 41.84 average 32.07	5	Medium-grained sandstones Fine-Grained sandstones Coarse-grained sandstone	24.72 - 27.87 average 26.63	1.28	Medium development	28	6.07	0 - 170	Moderately stable

6. Field Application

6.1. Support Program

The perimeter rock stability class of the 18-coal roadway in Baliancheng coal mine belongs to Class III, i.e. medium stable perimeter rock. To enhance the stability of the surrounding rock, the original support scheme was optimized based on borehole camera observations of the roof. The results indicated that fracture concentration zones were predominantly within 2.16 m of the roadway roof. Consequently, the roof bolt length was increased from 2000 mm to 2200 mm. Field investigations revealed rock fall occurrences between bolts, prompting an increase in bolt density from 6 to 7 per row. Additionally, field measurements showed roof subsidence ranging between 170 - 190 mm. Considering the maximum elongation of anchor cables (3%) and the design principle that anchor cable length should be 1.5 times the roadway span, the anchor cable length was extended from 6500 mm to 7300 mm, and the number per row was increased from 2 to 3. For the rib support, the bolt length was extended from 1800 mm to 2000 mm, while the number and spacing remained unchanged. The optimized support scheme is illustrated in (Figure 7).

6.2. Support Effect Test

Surface displacement observation of the roadway perimeter rock was carried out

for 30 d under the present support scheme and the original support scheme, as shown in (Figure 8).

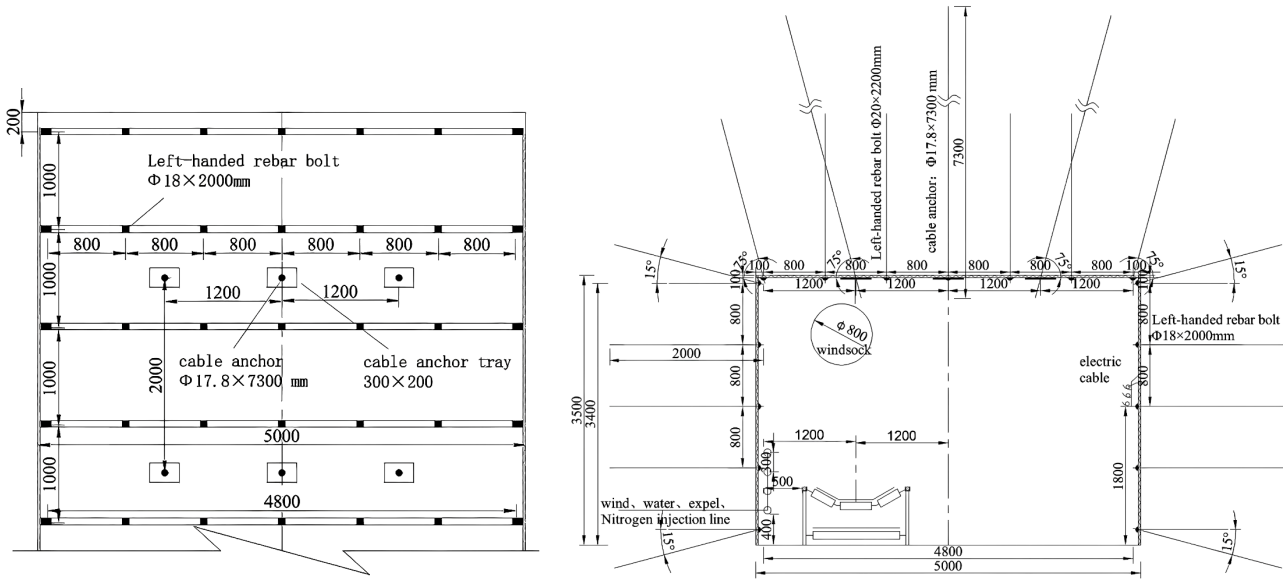

Figure 7. Cross-section and plan view of roadway support.

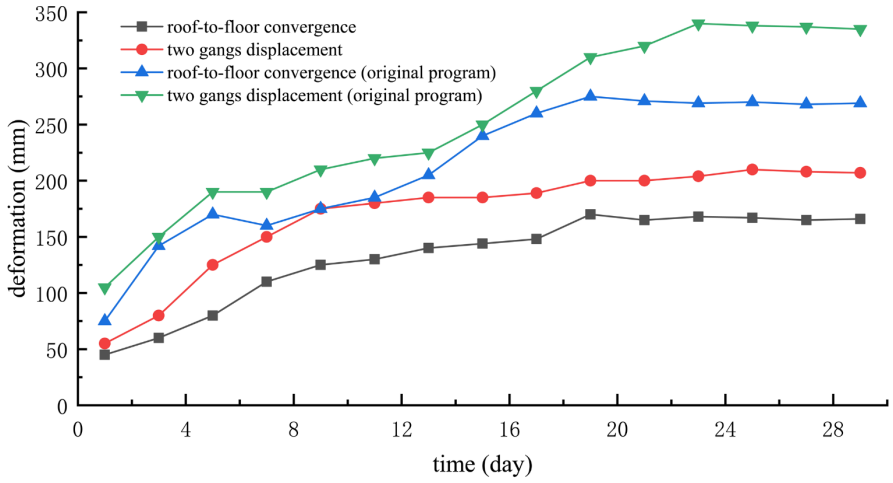

Figure 8. Comparison chart of surface displacement observations of surrounding rock in roadways.

From (Figure 8), it can be seen that under the present support scheme, the maximum displacement of the top and bottom plates of the roadway is 164 mm, and the maximum displacement of the two gangs is 283 mm, and the overall deformation of the roadway is relatively reduced compared with that of the original support scheme, and the support effect of the roadway surrounding rock is good.

7. Support Effect Test

1) The nine main influencing factors of roadway roof strength, coal seam strength, bottom plate strength, roadway depth, direct roof thickness to mining height ra-

tio, coal guard width, direct roof initial fall step, mining influence coefficient and stress ratio were determined as the classification indexes of roadway peripheral rock stability. The 18# coal roadway has a medium-hard composite roof of siltstone, medium-grained sandstone, and Coarse-grained sandstone, a soft-to-medium-hard composite floor of medium-grained, fine-grained, and coarse sandstone, a coal seam firmness coefficient of 1.28, a mining influence coefficient of 2.71, coefficient of lateral pressure of 1.90.

2) A comprehensive index method for classification of roadway rock stability was proposed, and combined with the classification results of the stability of the roadway rock in gently sloping and inclined coal seam back mining, the stability of the roadway rock was evaluated comprehensively and quantitatively, and an optimized support scheme was designed based on the classification results.

3) The stability class of 18-coal roadway in Baliancheng coal mine belongs to Class III, i.e. medium stability rock, and the overall deformation of the roadway is relatively reduced by the optimized support scheme, and the roadway rock support effect is good. The classification results and optimized support schemes are only applicable to coal seams and roadways in mines with similar geological conditions.

Conflicts of Interest

The authors declare no conflicts of interest regarding the publication of this paper.

References

Bai, D. D., Ji, Z., Li, P. et al. (2020). Evaluation and Prevention Technology of Island Risk Comprehensive Index Method in Semi Island Working Face. *Coal Science and Technology, 48,* 188-193.

Cao, R. G., & Hu, X. B. (2024). Discussion on Stability Analysis and Classification Method Improvement of Soft Red-Bed Rock Mass. *Water Conservancy and Hydropower Engineering Design, 43,* 33-36.

Cheng, H. B., & Wu, C. (2022). Analysis of Surrounding Rock Stability and Key Influencing Factors in the Goaf Area of Special-Shaped Roadway. *China Mining Magazine, 31,* 102-110.

Dong, E. Y., Yuan, C., Li, M. et al. (2023). Study on Stability Analysis and Anchorage Optimization Design of Sur-rounding Rock in Soft Rock Roadway. *Coal Technology, 42,* 54-58.

Feng, R. G. (2022). *Stability Analysis of Surrounding Rock in Deep Roadway under Complex Stress Field*. Hebei University of Engineering.

Hou, C., Jiang, L., Guo, L. et al. (1997). High-Strength Anchor Rod. *Ground Pressure and Strata Control Coal tunnel Anchor Support, 1,* 179-182+234.

Lan, H., Zheng, L. L., Chen, Q. G. et al. (2022). Stability Analysis of Roadway Surrounding Rock with Weak Interlayer under Dynamic and Static Loads. *Safety in Coal Mines, 53,* 241-246+252.

Li, G. C., Yang, S., Sun, Y. T. et al. (2022). Research Progress of Roadway Surrounding Strata Rock Control Technologies under Complex Conditions. *Coal Science and Technology, 50,* 29-45.

Lian, X. Y., Li, J., Wu, Z. et al. (2023). Study on Fuzzy Cluster Analysis of Roadway Surrounding Rock Failure Theory. *China Coal, 49,* 37-45.

Wang, Y. S. (2015). *Intelligence Research on Classification of Roadway Surrounding Rock Stability and Supporting Decision*. Anhui University of Science and Technology.

Wei, J. P., Li, Z. C., & Sang, P. M. (2010). Classification on Surrounding Rock Stability of Mining Gateway Base on Fuzzy Comprehensive Judgment. *Coal Engineering, 5,* 69-72.

Xu, Z. H., & Li, X. B. (2020). Evaluation and Application of Roadway Surrounding Rock Stability. *Coal Technology, 39,* 25-28. https://doi.org/10.13301/j.cnki.ct.2020.05.008

Yang, Z. H., & Liu, H. W. (1999). Artificial Neural Network Model for the Stability Classification of Adjoining Rock of Underground Construction. *Journal of Archives Sichuan University, 4,* 66-72.

Zhang, P. S., Xu, D. Q., Zhang, X. L. et al. (2023). Multi-Factor Influence Index Analysis and Prediction of Failure Depth of Coal Seam Floor. *Journal of Mining & Safety Engineering, 5,* 5-15. https://doi.org/10.13532/j.jmsce.cn10-1638/td.20221226.001

Zhang, T., Zhao, Y. X., Zhu, G.P. et al. (2016). A Multi-Coupling Analysis of Mining-Induced Pressure Characteristics of Shallow-Depth Coal Face in Shendong Mining Area. *Journal of China Coal Society, 41,* 287-296.

Zhao, J. H., Li, F. J., Liu, Y. Z. et al. (2024). Stability Analysis and Support Research of Shaft and Roadway Surrounding Rock Based on Key Blocks. *China Mining Magazine, 33,* 304-311.

Zheng, X. Z., & Yu, Y. X. (2014). Fuzzy Equivalent Clustering Analysis of Surrounding Rock Stability in Wangcun Mine. *Coal Geology & Exploration, 42,* 55-60.

Zhu, Y. J., Shi, H. Y., Wang, P. et al. (2015). Zhu Erlei1 Multiple Linear Regression Analysis on Affecting Factors of Tip-to-Face Roof Caving Height. *Journal of Hunan University of Science & Technology (Natural Science Edition), 30,* 1-6.